# Photochemical Reactions of Silylene with Ethene and Silene

**Ch. Lennartz, H. M. Hildebrandt, and B. Engels***

*Institut für Physikalische und Theoretische Chemie, Universität Bonn, Wegelerstrasse 12, D-53115 Bonn, Germany*

*Received: June 16, 1997; In Final Form: September 2, 1997*[⊗]

To obtain insight into the photochemical behavior of silylene ($SiH_2$), the reactions of silylene in its first two excited states ($^3B_1$, $^1B_1$) with ethene and silene are studied. The potential energy surfaces (PESs) governing these reactions are calculated by ab initio methods. Our calculations show that minima of the PES describing the reactions of $SiH_2(^1B_1)$ result from an avoided crossing between the two lowest singlet states. As a consequence, the products of these reactions possess quite unusual equilibrium geometries. Furthermore, using estimates based on the Landau−Zener model, we expect the internal conversion from the excited singlet states to the ground-state PESs to be very efficient. Hence the main final products of the reactions starting from the $^1B_1$ state will be thermally highly excited ground-state molecules. While the reactions of $SiH_2(^1B_1)$ are found to be strongly influenced by the electronic ground state, the reactions of the triplet states do not feature crossing with any of the singlet PESs in the vicinity of the minimum energy path. Furthermore our analysis allows us to rationalize the trends in the stabilization energies of the various reactions.

## 1. Introduction

Silylene is an important intermediate in the pyrolysis of silanes and is known to play a key role in the chemical vapor deposition (CVD) process to form thin films of amorphous silicon.[1] It is furthermore an important model compound for the investigation of the similarities and differences in the chemical properties of silicon and carbon. Due to the high reactivity of silylene, theoretical studies have proved to be crucial for the understanding of the chemical behavior of this compound. The three lowest-lying states are the $X^1A_1$ ground state, the $a^3B_1$ state, lying above the ground state by 18.4 kcal/mol, and the first excited singlet state, $A^1B_1$, being 46.8 kcal/mol above the ground state.[2] The similarity of the $^3B_1$ and the $^1B_1$ states is due to the occupation of the orbitals. While the $^1A_1$ ground state possesses a doubly occupied $5a_1$ and an empty $2b_1$ orbital, for the $^3B_1$ and the $^1B_1$ state both orbitals are singly occupied and the states only differ by the spin coupling. The energetic position of various higher excited states were calculated, among others, by Winter and Millie[3] and Rice and Handy.[4]

The reaction of $SiH_2(^1A_1)$ with ethene was studied by Anwari and Gordon.[5] They calculated the minimum energy path (MEP) of the reaction and discussed the reaction mechanism, which was found to be very similar to the analogous reaction of methylene. For the geometry optimization they used SCF gradients while total energies were obtained from single-point MP2/3-21G calculations. Recently Horner et al.[6] computed the stabilization energies of the various three-membered rings containing silicon, employing the CCSD approach in combination with an atomic orbital (AO) basis of double-$\zeta$ plus polarization quality. The geometries were optimized using SCF gradients. Experimentally the $^1A_1$ reaction was studied by Rogers et al.[7] Jasinski et al.[8] and Suzuki et al.[9] measured reaction rate constants using the transitions between the two lowest-lying singlet states of $SiH_2$ to monitor the silylene concentration. In a recent study, Walsh and co-workers[10] studied differences and similarities in the addition reactions of silylene and methylene to $C_2H_4$. Other studies, less related to the present work, can be found in the review of Apeloig.[11]

To the best of our knowledge no information about the photochemical reaction of silylene with ethene exists. In the present study this gap is closed by investigating the reactions of the two first excited states of silylene ($^3B_1$,$^1B_1$) with ethene. Like the analogous reaction involving methylene, the $SiH_2(^3B_1) + C_2H_4$ reaction is expected to lead to a biradical, open-chain product. Due to the similarities in the orbital occupation of the $^3B_1$ and the $^1B_1$ states, we expect a similar product for the $SiH_2(^1B_1) + C_2H_4$ reaction. One motivation for our studies is that secondary reactions starting from such biradical open-chain products could be useful for the synthesis of silicon−hydrogen networks.

In addition to the reactions with ethene, we also studied the reactions of silylene with silene ($H_2C{=}SiH_2$) to investigate the differences resulting from the formation of silicon−silicon bonds, the influence of the much weaker double bond of silene, and the effect of the dipole moment of silene.

The present paper is divided into three parts. After a description of the technical details, the potential energy surfaces (PESs), and the reaction mechanisms of the various reactions are given. In the third part of the paper the results will be used to discuss the differences in the appropriate methylene reactions and to rationalize trends with a model introduced by Horner et al.[6] Furthermore we consider the photochemical relevance of the $^1B_1$ reaction using the Landau−Zener approach, which allows us to analyze possible intersystem crossings which may influence the triplet reactions.

## 2. Technical Details

All calculations were performed in $C_s$ symmetry since test calculations made without any symmetry constraints turned out to give the same optimized geometries. In the reactions studied in the present work, ethene and silene are in their electronic ground states $^1A_{1g}$ and $^1A_1$, respectively. Therefore the symmetry and the spin of the electronic states of the reaction products are determined by the silylene fragment. Due to the $C_s$ symmetry, the educt channels starting from the $X^1A_1$ and the $A^1B_1$ state of the silylene fragment correlate with the two lowest-lying $^1A'$ electronic states of the products $Si_2CH_6$ and $SiC_2H_6$, while the addition of triplet silylene ($a^3B_1$) to ethene

* To whom correspondence should be addressed.
[⊗] Abstract published in *Advance ACS Abstracts,* November 1, 1997.

S1089-5639(97)01957-9 CCC: $14.00 

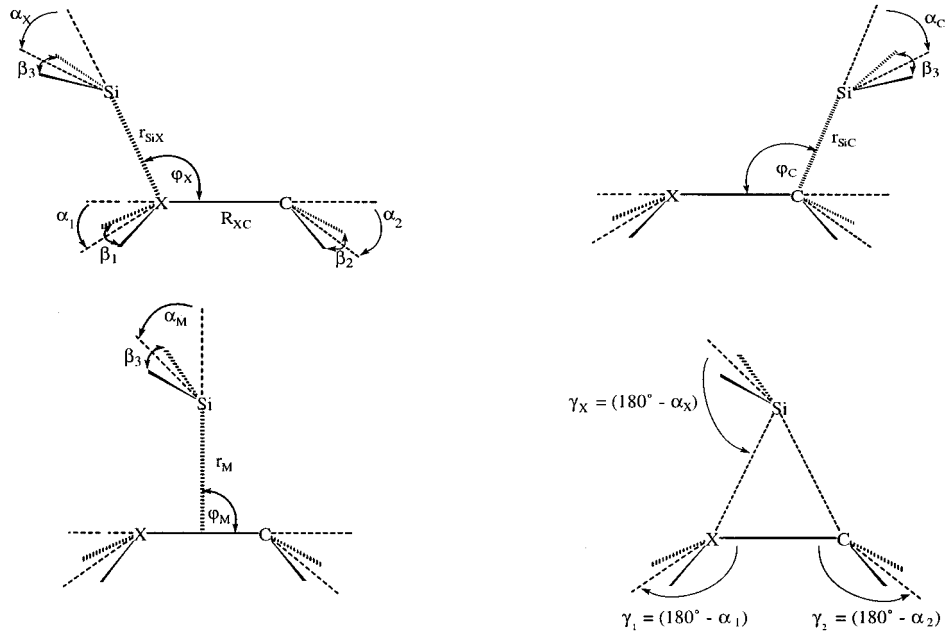


**Figure 1.** Structural parameters used for geometry optimization. The upper part shows $r_{SiX}/r_{SiC}$ and $\varphi_X/\varphi_C$ defining the position of the silicon center of the silylene fragment with respect to the attacked center (X = C, ethene; X = Si, silene). On the left side of the lower part $r_M$ and $\varphi_M$ are shown, which were useful for the optimization of the MEP of the $^1A_1$ reactions. Additional parameters used for the description of the $^1A_1$ minimum are given on the right side of the lower part ($\gamma_X$, $\gamma_1$, $\gamma_2$).

or silene leads to the lowest triplet state of the product compounds ($^3A'$). To emphasize the connection between the reactions and the different electronic states of the silylene fragment, the reactions will be classified in accordance with the nomenclature for the electronic states of silylene, e.g., the reaction starting from the $X^1A_1$ state of silylene will be referred to as the $^1A_1$ reaction while the two other reactions will be called $^3B_1$ and $^1B_1$ reactions.

The geometrical parameters used in the present study are shown in Figure 1. The PESs of the reactions are obtained by fixing the primary parameters at certain angles and distances and optimizing all secondary parameters for each pair of primary parameters.

Two different sets of primary parameters are employed for the description of the various reactions. In the first one (set A, upper part of Figure 1), the parameters $\varphi_C/\varphi_X$ and $r_{SiC}/r_{SiX}$ are the primary parameters. They define the position of the silicon center of the silylene fragment with respect to the attacked carbon center in the case of ethene (X = C). In silene (X = Si) two different centers, C and Si, can be attacked. Therefore for the silene reactions set A was used in two versions, describing the approach to the carbon ($r_{SiC}$, $\varphi_C$) and the silicon center ($r_{SiSi}$, $\varphi_{Si}$), respectively. In the second set of primary parameters (set B, lower left part of Figure 1) the silicon center of silylene is related to the middle of the X−C bond, using $r_M$ and $\varphi_M$ as parameters.

For the optimization of the secondary parameters we used a CAS-SCF energy gradient. The active space of the CAS-SCF computations[12] consisted of six electrons distributed among six orbitals, namely the $5a_1$ and $2b_1$ MOs of the silylene fragment and the $\sigma$, $\pi$, $\pi^*$, and $\sigma^*$ MOs of the ethene and silene fragments, respectively. Due to root-flipping problems occurring in the CAS-SCF calculations of the $2^1A'$ state, the secondary parameters for the $^1B_1$ reaction could not be optimized with analytical energy gradients. Therefore a grid scheme was used to optimize the most important secondary parameters $\varphi_C$, $R_{CC}$, $\alpha_C$, $\alpha_2$, $\alpha_3$, $\beta_1$, and $\beta_3$ for the reaction with ethene and $R_{CSi}$, $\alpha_{Si}$, $\alpha_2$, $\alpha_3$, $\beta_1$, $\beta_3$, and $\varphi_{Si}$: or $\varphi_C$ for the reaction with silene. For this optimization, the energy was calculated with the internally contracted multireference CI method[13] employing state-averaged CAS-SCF natural orbitals. In these calculations, six electrons of the CAS space were correlated. This kind of calculation will be referred to as MR-CI(6).

The $1^1A'$ and $^3A'$ PESs single-point calculations using the MR-CI(6) approach were performed for each optimized geometry, and final stabilization energies and barrier heights were obtained by internally contracted MR-CI calculations in which all 18 valence electrons were correlated. In the following, these computations will be referred to as MR-CI(18) calculations. For the calculations described above the MOLPRO program package[14] was employed. The accuracy of the calculations was checked by computations using even larger reference spaces employing the individually selecting MRD-CI method.

For the calculations described above two different sets of Gaussian basis functions were employed. For the geometry optimization and the calculation of the PES we employed the split-valence 6-31G** basis set which includes d-type polarization functions on the heavier centers and p-type polarization functions on hydrogen.[15] Final stabilization energies and barrier heights were computed using the valence triple-$\zeta$ 6-311G** basis set[16] in combination with the MR-CI(18) approach. To estimate the influence of basis set extensions on the thermochemical properties, the G2 method[17] was employed to compute the stabilization energies of the various products.

## 3. Description of Potential Energy Surfaces and Reaction Mechanisms

The PESs of the $^1A_1$ and the $^3B_1$ reactions and the MEP of the $^1B_1$ reactions are presented in Figures 2, 3, 4, and 6−9 while the characteristic energies (stabilization energies and barrier heights of the MEP) are given in Table 1. The geometrical parameters of the products are shown in Table 2.

**Reactions of Silylene with Ethene.** *The $^3B_1$ Reaction ($SiH_2(^3B_1) + C_2H_4$).* The PES of the $^3B_1$ reaction, characterized by cuts for $\varphi_C$ = 150°, 130°, 110°, and 90°, by the MEP, and by the cut for $\varphi_M$ = 90°, is given in Figure 2.

The $^3B_1$ reaction leads to an open-chain product ($\varphi_C$ = 115°, $r_{SiC}$ = 1.96 Å) with a calculated stabilization energy of 16 kcal/

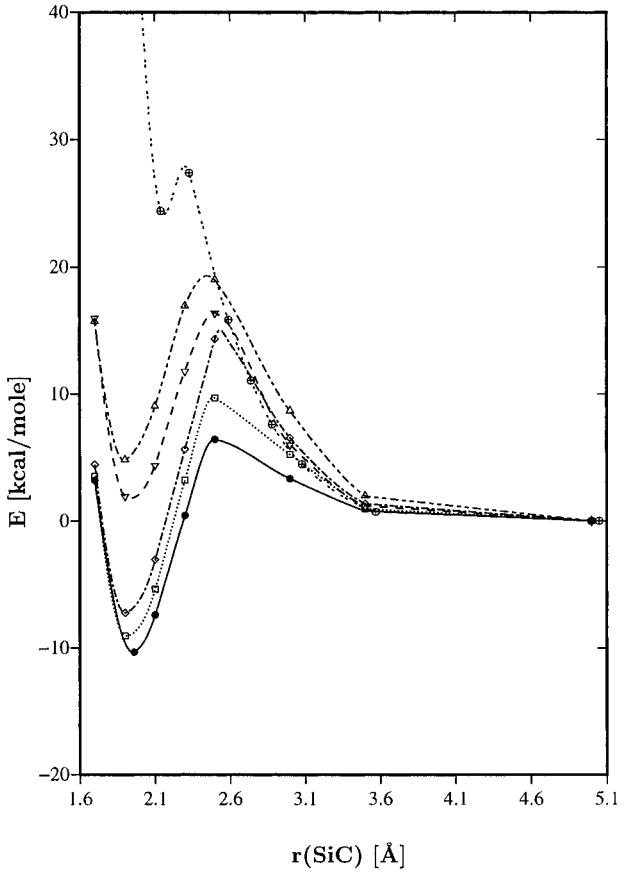


**Figure 2.** PES of the $^3B_1$ reaction $SiH_2(^3B_1) + C_2H_4$ characterized by the cuts for $\varphi = 150°$ (△), 130° (◇), 110° (□) and 90° (▽). Additionally, the MEP (●) and the cut for $\varphi_M = 90°$ (⊕) is given. The PES was calculated using the MR-CI(6) approach. It should be kept in mind that the barrier heights and the stabilization energies change slightly if the improved MR-CI(18) approach is employed.

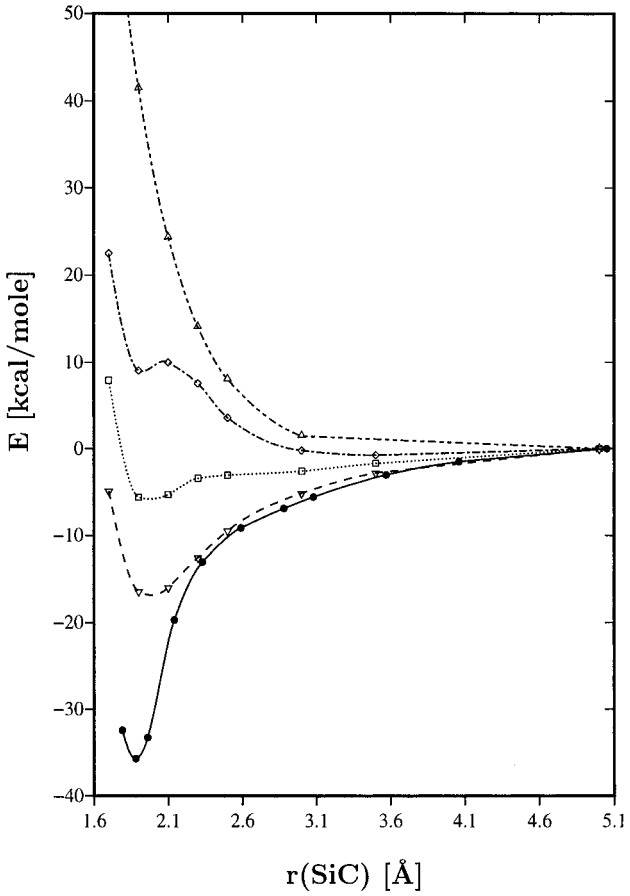


**Figure 3.** PES of the $^1A_1$ reaction $SiH_2(^1A_1) + C_2H_4$ characterized by the cuts for $\varphi = 150°$ (△), 130° (◇), 110° (□) and 90° (▽). In addition, the cut for $\varphi_M = 90°$ (●), which is identical to the MEP, is plotted. For more information see Figure 2.

mol (MR-CI(18) approach). Employing the G2 theory and including zero-point energy corrections, a value of 14 kcal/mol is obtained. The reaction is hindered by a small barrier predicted as 2 kcal/mol (MR-CI(18) approach). The product possesses biradical character with one electron centered at each terminal group. In analogy to the geometries of $SiH_3$ (pyramidal structure) and $CH_3$ (planar structure), the terminal silicon atom has a pyramidal coordination ($\alpha_C = 54°$, $\beta_3 = 109°$), while the terminal carbon atom possesses a nearly planar coordination ($\alpha_C = 18°$, $\beta_3 = 117°$).

The double bond of the ethene fragment is broken ($R_{CC}$ = 1.52 Å) and the hybridization at the attacked carbon atom has changed from $sp^2$ to $sp^3$ hybridization ($\beta_2 = 108°$). Two isomers of the product exist. They represent the two possible inclinations of the $SiH_2$ group. Isomer I has $\alpha_C = -51°$ while isomer II has $\alpha_C = +51°$. They are very similar in energy ($\Delta_E < 1$ kcal/mol) but are separated by a barrier of 10 kcal/mol ($\alpha_C = 0°$). Depending on the starting value of the inclination angle $\alpha_C$, isomer I or isomer II is formed.

In the PES, a sharp increase of the energy is found for $\varphi_C < 110°$, resulting in a nearly repulsive cut for $\varphi_M = 90°$. Therefore the 1,2-migration motion of the silylene fragment cannot take place but leads to dissociation into the fragments. On the other hand, the cut for $\varphi_C = 130°$ is only destabilized by 3 kcal/mol.

As described for the addition of methylene to ethene,[18] the first step of the $^3B_1$ reaction (up to $r_{SiC} = 2.5$ Å) is characterized by an electrophilic attack of silylene on the $\pi$ system of the ethene fragment. At $r_{SiC} = 2.3$ Å, the new Si−C bond begins to be formed and the charge transfer of the first step is reversed. This is accompanied by the opening of the double bond and a change from $sp^2$ to $sp^3$ hybridization at the attacked carbon atom. During the whole reaction the angle $\varphi_C$ differs only slightly from 115°.

*The $^1A_1$ Reaction ($SiH_2(^1A_1) + C_2H_4$).* The shape of the PES of the $^1A_1$ reaction is visualized in Figure 3 by the cuts for the $\varphi_C = 90°$, 110°, 130°, and 150°. In addition, the cut for $\varphi_M = 90°$, which is identical to the MEP, is plotted.

As known from the work of Anwari and Gordon,[5] the $SiH_2(^1A_1) + C_2H_4$ reaction represents a barrierless process because the symmetry-forbidden least-motion $C_{2v}$ attack can be circumvented. In the present work, the stabilization energy of the product silacyclopropane is calculated as 44 kcal/mol, employing the MR-CI(18) approach, and 42 kcal/mol if the G2 theory is used. Using the MP2 method in combination with a 3-21G basis set, Anwari and Gordon[5] obtained a stabilization energy of around 31 kcal/mol. Horner et al.,[6] using the CCSD/DZP method, computed a stabilization energy of 48 kcal/mol. The equilibrium geometries of rings containing silicon were already discussed several times[6,19] but only SCF optimization was performed. As is to be expected, our CAS-SCF optimizations lead to somewhat longer bonds for $r_{SiC}$ (1.88 vs 1.86 Å) and $R_{CC}$ (1.59 vs 1.55 Å).

A short comment upon the shape of the $^1A_1$ PES is of interest because Anwari and Gordon only discussed the MEP of the $^1A_1$ reaction. From the cuts through the PES (Figure 3) it is seen that repulsive interactions between the silylene and ethene fragments are only found for large values of $\varphi_C$ ($\varphi_C > 110°$) while for smaller values of $\varphi_C$ the approach of silylene to ethene represents a barrierless process. Nevertheless, the energy

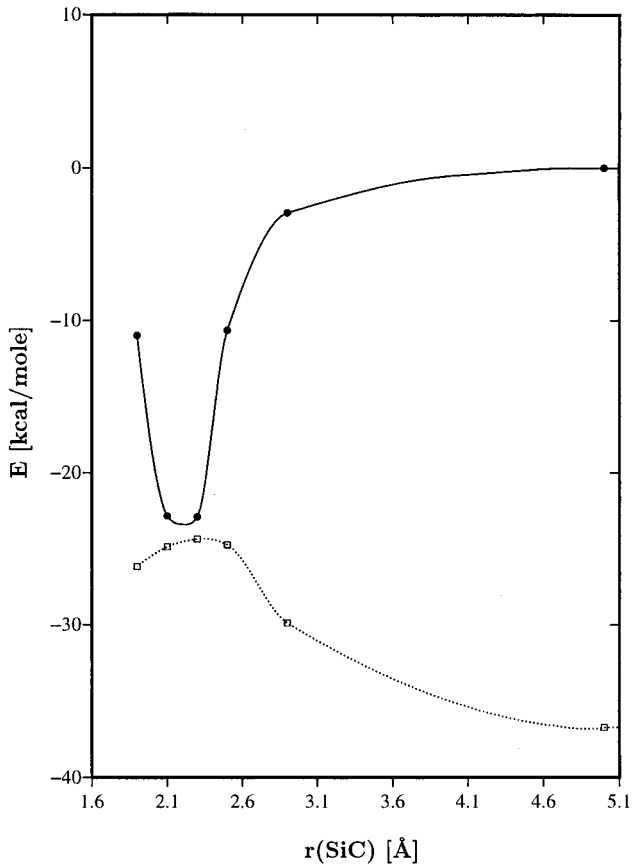


**Figure 4.** Energies of the $1^1A'$ (□) and $2^1A'$ states (●) for the $SiH_2$-($^1B_1$) + $C_2H_4$ reaction along the minimum energy path of the $2^1A'$ state. The energies were computed with the MR-CI(18) approach.

increases sharply if the silacyclopropane undergoes a ring-opening reaction.

For a description of the reaction mechanism, which is very similar to the equivalent methylene reaction,[18,20] the reader is referred to the literature.[5]

*The $^1B_1$ Reaction ($SiH_2(^1B_1)$ + $C_2H_4$).* Due to the $C_s$ symmetry of the reaction complex, the PES governing the $SiH_2$-($^1B_1$) + $C_2H_4$ reaction represents the first excited $^1A'$ surface ($2^1A'$). The MEP of the $^1B_1$ reaction is plotted in Figure 4. At large $r_{SiC}$ distances, the electronic configuration of the surface can be described as [...]$11a'^2 12a'^1 13a'^1$, i.e., it possesses two open shells corresponding to the singly occupied $a_1$ and $b_1$ orbitals of the silylene fragment. The 11a′ orbital represents the $\pi$ orbital of the ethene fragment.

The $^1B_1$ reaction is found to proceed without a barrier leading to an open-chain product with a stabilization energy of about 23 kcal/mol. The minimum of the $2^1A'$ PES lies 69 kcal/mol above the minimum of the silacyclopropane ground state and at 22 kcal/mol above the minimum calculated for the $^3B_1$ reaction. The minimum of the MEP of the $^1B_1$ reaction is determined at $\varphi_C = 100°$ and $r_{SiC} = 2.2$ Å. Both values differ from their counterparts (115°, 1.96 Å) of the $^3B_1$ reaction. The Si−C bond length of 2.2 Å is substantially longer than a normal Si−C single bond (1.9 Å), and the optimized C−C bond length of 1.47 Å is shorter than a C−C single bond (1.54 Å). The energy of the $2^1A'$ state is very sensitive to the variation of $\alpha_C$. At the minimum it has a value of 110°, which is distinctly larger than that for the minimum of the $^3B_1$ reaction ($\alpha_C = 61°$). The unexpected geometrical structure results from an avoided crossing between the two lowest states taking place at the minimum of the MEP of the $^1B_1$ reaction. As a consequence, for $r_{SiC} = 2.2$ Å and $\varphi_C = 100°$ the electronic character of the first excited $^1A'$ state changes to the electronic configuration of the former ground state ([...]$11a'^2 12a'^2$) while the electronic character of the ground state turns into [...]$11a'^1 12a'^1 13a'^1$, i.e., for $r_{SiC} < 2.3$ Å and $\varphi_C > 100°$ the ground state possesses an open-shell structure.

The reasons for the avoided crossing between the ground and the excited state, namely the destabilization of the closed-shell configuration [...]$11a'^2 12a'^2$ and the stabilization of the open-shell configuration [...]$11a'^2 12a'^1 13a'^1$, are connected with the character of the orbitals 11a′−13a′. The change in the shape of the orbitals in the course of the reaction is displayed in Figure 5. In the fragmentation channel (5.0 Å) 11a′ represents the $\pi$ orbital of the ethene fragment, while 12a′ and 13a′ are the $a_1$ and $b_1$ orbitals of the silylene fragment. In the course of the reaction the $b_1$ orbital of the silylene fragment (13a′) overlaps with the $\pi$ orbital of ethene (11a′), forming a bonding (new 11a′) and a mainly nonbonding orbital (new 13a′). The form of the 13a′ orbital results from additional mixing with the $\pi^*$ orbital of the ethene fragment. The bonding linear combination represents the newly formed Si−C bond, while the nonbonding orbital corresponds to the remaining part of the $\pi$ orbital and is mainly located at the terminal carbon center. The character of the 12a′ orbital remains nearly unchanged, i.e., it preserves the orbital character of the silylene fragment. For the closed-shell configuration [...]$11a'^2 12a'^2$, in the course of the reaction, charge is moved from the terminal carbon center into the newly formed Si−C bond (11a′). Due to this charge transfer at $r_{SiC} \leq 2.3$ Å, the closed-shell configuration is a strongly polarized complex because in the course of the reaction charge is moved from the terminal $CH_2$ group into the newly formed Si−C bond as can be seen from the shape of the 11a′ orbital. If the 12a′ and 13a′ orbitals are singly occupied, the charge transfer occurring due to the changes in the 11a′ orbital is compensated for by the rearrangements found in the 13a′ orbital. Therefore, the open-shell configuration always describes a homogeneous electron distribution over the whole molecule. For the closed-shell configuration, an additional destabilization results from the fact that formally negative charge is transferred from the terminal carbon center to the silicon center, the latter being less electronegative. The effect of the charge accumulation is clearly revealed by the changes of the dipole moments of both states along the MEP of the $^1B_1$ reaction. A strong increase of the dipole moment is found for the diabatic state which is connected with the closed-shell configuration while the dipole moment of the diabatic state dominated by the open-shell configuration remains nearly constant.

For both configurations a new Si−C single bond is formed while the C−C $\pi$ bond is weakened. The bonding situation at the minimum of the excited state ($r_{SiC} = 2.3$ Å, $\varphi_C = 100°$) may be characterized as a charge-transfer complex, where a $^1A_1$ silylene is coordinated to the $\pi$ system. The bonding results from a charge transfer from the $\pi$ system to the empty $2b_1$ orbital of silylene.

The open-chain geometry of the ground state is much higher in energy than the cyclic form, which represents the equilibrium geometry. Going from the open-chain form to the cyclic form, the orbitals 12a′ and 13a′ combine to form the second Si−C bond of silacyclopropane. As a consequence, a reorganization of the electronic structure takes place, which again stabilizes the closed-shell configuration. Therefore, another avoided crossing is found if one moves from $\varphi_C = 100°$, $r_{SiC} = 2.1$ Å to smaller values of $\varphi_C$.

**Reactions with Silene.** Differences of the reactions with silene compared to ethene are due to several aspects: First, there is the possibility to form a symmetric ($SiH_2$−$CH_2SiH_2$) and an

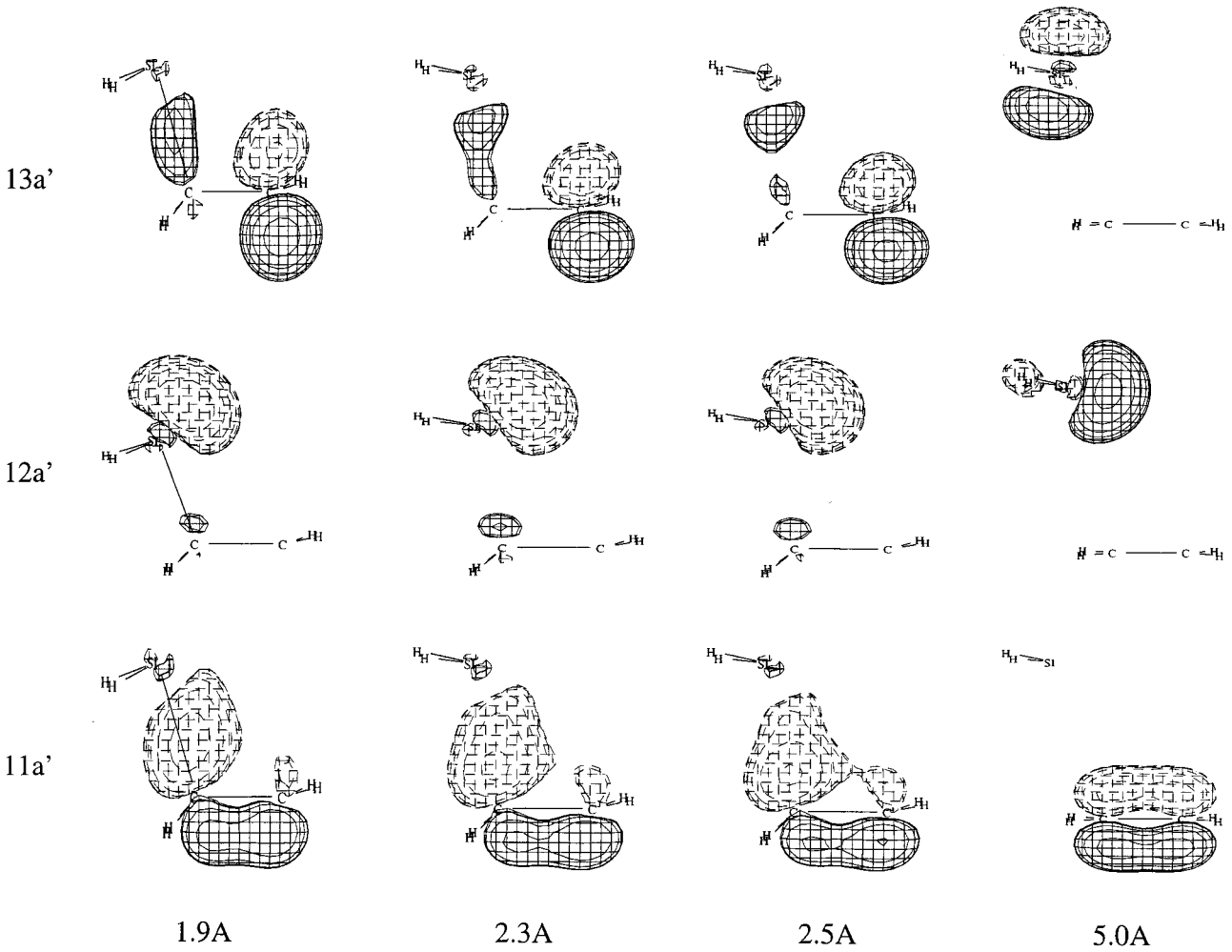


**Figure 5.** Change in the character of the 11a′−13a′ orbitals in the course of the $SiH_2(^1B_1) + C_2H_4$ reaction. The $r_{SiC}$ distances are indicated.

asymmetric product ($CH_2SiH_2-SiH_2$). Furthermore, the $\pi$ bond of silene is weaker, and the dipole moment of silene does not vanish as it does in case of ethene.

In the following subsections the PES and the reaction mechanism of the various reactions will be described.

*The $^3B_1$ Reaction ($SiH_2(^3B_1) + CH_2SiH_2$).* The shape of the PES obtained for the $^3B_1$ reaction is given in Figure 6. The figure shows cuts for fixed $\varphi_C = 130°$, 90° as well as the MEP, describing the attack of silylene at the carbon center and cuts for fixed $\varphi_{Si} = 130°$, 80° and the MEP characterizing the addition to the silicon center of silene. Using the MR-CI(18) method, the barriers computed by the MR-CI(6) approach shown in Figure 6 are not confirmed, i.e., our study predicts that both reactions are barrierless processes.

Using the MR-CI(18) method the stabilization energy for the symmetric product is found to be 46 kcal/mol, while 37 kcal/mol is computed for the asymmetric product. If the G2 theory is employed, 45 and 39 kcal/mol, respectively, are calculated. As seen from Figure 6 the 1,2-shift process does not lead to a fragmentation, but starting from the asymmetric product a high barrier of more than 30 kcal/mol is calculated.

Due to the pyramidal coordination of the terminal silicon centers, the symmetric product possesses three different isomers. Isomer I possessing $C_{2v}$ symmetry is characterized by $\alpha_C = \alpha_1 = +51°$, isomer II represents the geometry with $\alpha_C = -\alpha_1 = +51°$, while isomer III, again possessing $C_{2v}$ symmetry, is characterized by $\alpha_C = \alpha_1 = -51°$. The energy differences between the isomers are very small (<1 kcal/mol) but the barrier heights of the isomerizations reactions ($\alpha_C = 0°$ or $\alpha_1 = 0°$) are at approximately 10 kcal/mol. Depending on the starting value of the inclination angle $\alpha_C$, isomer II or isomer III is formed but never isomer I.

For the asymmetric product only two isomers exist because the carbon center possesses a planar coordination. As for the symmetric product, both are very similar in energy. The isomerization barrier of 4 kcal/mol, which is considerably smaller than the isomerization barriers computed for the symmetric product, can be rationalized because electropositive substituents stabilize the planar form of $R-SiH_2$. Depending on the $\alpha_{Si}$ angle during the reaction, both isomers can be found.

Although the shape of the PES of the $^3B_1$ reaction with silene differs in various aspects from the corresponding ethene PES (no barrier for the addition process, 1,2-migration), the reaction mechanisms are found to be identical.[21] Therefore we will not go into a further discussion.

*The $^1A_1$ Reaction ($SiH_2(^1A_1) + H_2CSiH_2$).* The shape of the PES of the $^1A_1$ reaction is indicated in Figure 7, which gives the cuts for $\varphi_C = 80°$, 120° and $\varphi_{Si} = 90°$, 120°. In addition the MEP is plotted.

Up to $r_{CSi} = 2.39$ Å the MEP is identical with the cut for $\varphi_M = 90°$. For $r_{SiC} < 2.3$ Å the silylene fragment shifts toward the carbon atom forming the cyclic product which possesses $C_{2v}$ symmetry. The minimum is found for $\varphi_M = 73°$, $r_{CSi} = 1.94$ Å, and $r_{SiSi} = 2.30$ Å. The characteristic angles of the cyclic product are $\angle(SiSiC) = 54°$ and $\angle(SiCSi) = 73°$. The optimized bond lengths differ to some extent from the values given by Boatz and Gordon[19] ($r_{CSi} = 1.92$ Å, $r_{SiSi} = 2.26$ Å) who used SCF gradients only. Explanations for the unusually

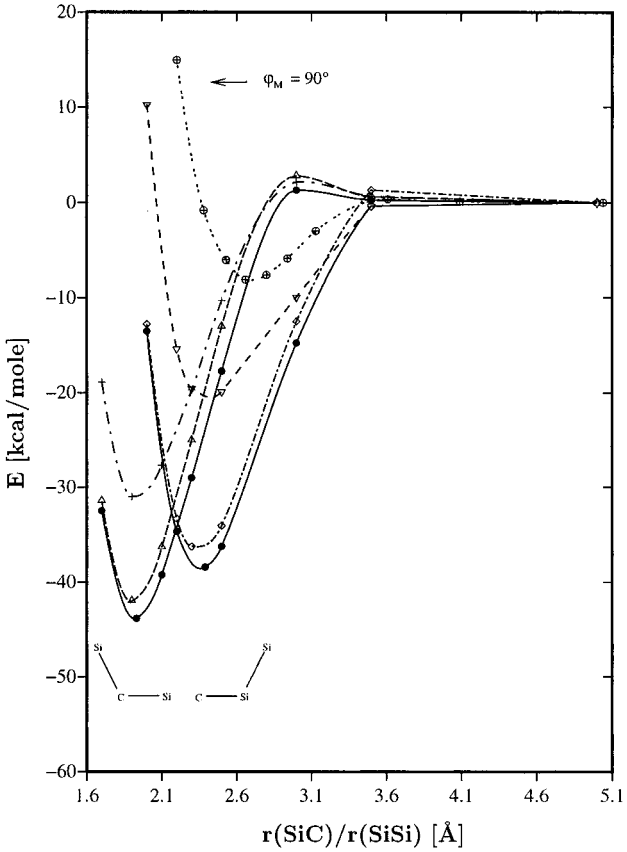


**Figure 6.** PES of the $^3B_1$ reaction $SiH_2(^3B_1) + CH_2SiH_2$ characterized by the cuts for $\varphi_C = 130°$ (△), 90° (+), and the MEP (●), describing the attack of silylene at the carbon center, and cuts for $\varphi_{Si} = 130°$ (◇), 80° (▽), and the MEP (●), characterizing the addition of silylene to the silicon center of silene. In addition $\varphi_M = 90°$ (⊕) is given. For more information see Figure 2.

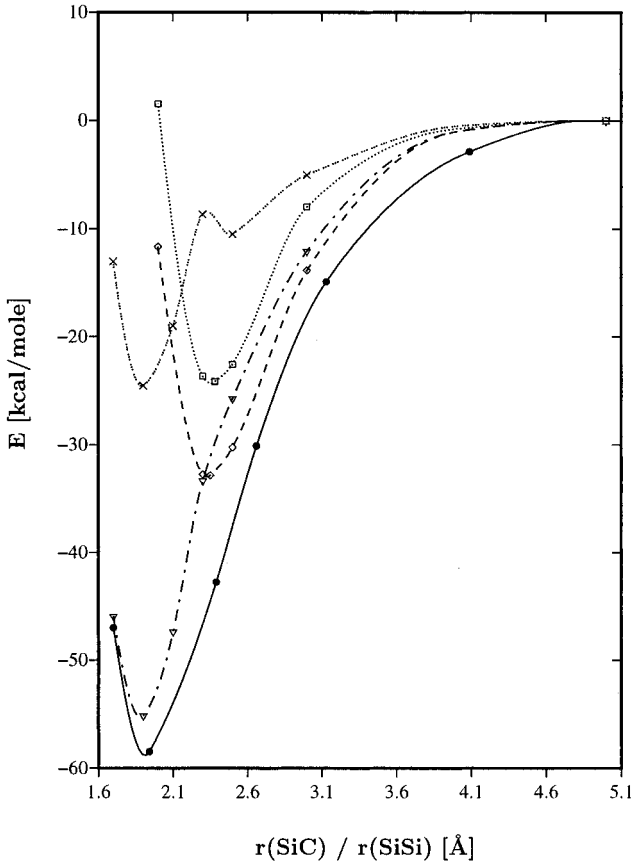


**Figure 7.** PES of the $^1A_1$ reaction $SiH_2(^1A_1) + CH_2SiH_2$ characterized by the cuts for $\varphi_C = 80°$ (▽) and 120° (×) and $\varphi_{Si} = 90°$ (◇) and 120° (□). In addition, the MEP (●) is plotted. For more information see Figure 2.

short SiSi bond were reviewed by Apeloig.[11] Both the MR-CI(18) approach and the G2 theory predict a stabilization energy of 61 kcal/mol, which is identical to the value given by Horner et al.[6]

As expected, the reaction is found to be a barrierless process. The reaction mechanism is analogous to the reaction of silylene with ethene.

*The $^1B_1$ Reaction ($SiH_2(^1B_1) + CH_2SiH_2$).* Like the $^3B_1$ reaction, the $^1B_1$ reaction leads to two open-chain products. The MEPs of the $^1B_1$ reaction are outlined in Figures 8 and 9. As for the reaction with ethene, no barrier is found for the present reaction and the minima of the PES are computed at fairly large C−Si (2.3 Å) and Si−Si distances (2.6 Å) with $\varphi_C = 110°$ and $\varphi_{Si} = 96°$. The stabilization energies are 43 kcal/mol for the $SiH_2-CH_2SiH_2$ isomer and 37 kcal/mol for the $CH_2SiH_2-SiH_2$ isomer. Although the stabilization energy is nearly doubled in comparison to our results for the $SiH_2(^1B_1) + C_2H_4$ reaction, the reaction mechanism and the reasons for the avoided crossings between the two lowest $^1A'$ states are identical.

**Discussion of Thermochemical Properties.** The stabilization energies and the barrier heights computed for the various reactions are summarized in Table 1. The table contains the computed stabilization energy of the reaction using the MR-CI(18) approach in combination with a 6-311G** AO basis set ($\Delta E$), and the G2 theory[17] in which the zero-point energy correction is included ($\Delta E^{G2}(0K)$). From the literature we added the values obtained by Horner et al.,[6] who used the CCSD method in combination with a 6-31G* AO basis set. Other results (see ref 11 for a review) are omitted because Horner et al. used the most reliable approach to date. In addition estimates obtained from a model explained below are given ($\Delta E^{est}$). The barriers for the various reactions computed on the MR-CI(18)/6-311G** level are also summarized. As shown in Table 1, the stabilization energies of all reactions of silylene with silene are higher than those of the corresponding reactions of silylene with ethene, and as already discussed for the $^1A_1$ species,[6,10] methylene reactions are more exothermic than the corresponding silylene reactions. Furthermore, while barriers are computed for the $^3B_1$ reactions with ethene, both possible $^3B_1$ reactions of silylene with silene are predicted to be barrierless processes.

Before discussing trends found in the stabilization energies of the various reactions, a comment upon the accuracy of the calculated values is necessary. As shown for a large number of first- and second- row compounds, the error in the G2 theory for atomization energies is around 1−2 kcal/mol. The accuracy for the silicon compounds studied in the present work can be estimated from the computed values of the singlet−triplet gap of silylene, for which very accurate calculations were performed by Bauschlicher et al.[22] The G2 theory, without including zero-point corrections, predicts a singlet−triplet gap of 23.4 kcal/mol, which lies about 3 kcal/mol above the best theoretical value of 20.6.[22] Subtracting the influence of the nuclear motion, an experimental value of 20.7 kcal/mol is found.[23]

An error source in the G2 value is the estimation of the influence of the basis set size, which within the G2 theory is estimated to be 2.8 kcal/mol, while the work of Bauschlicher et al. gives an influence of only 0.8 kcal/mol.

A second error source is the empirical higher level correction which should account for deficiencies in the treatment of the electron correlation. In the G2 theory, the higher level corrections are added to the QCISD(T) result. Therefore the accuracy

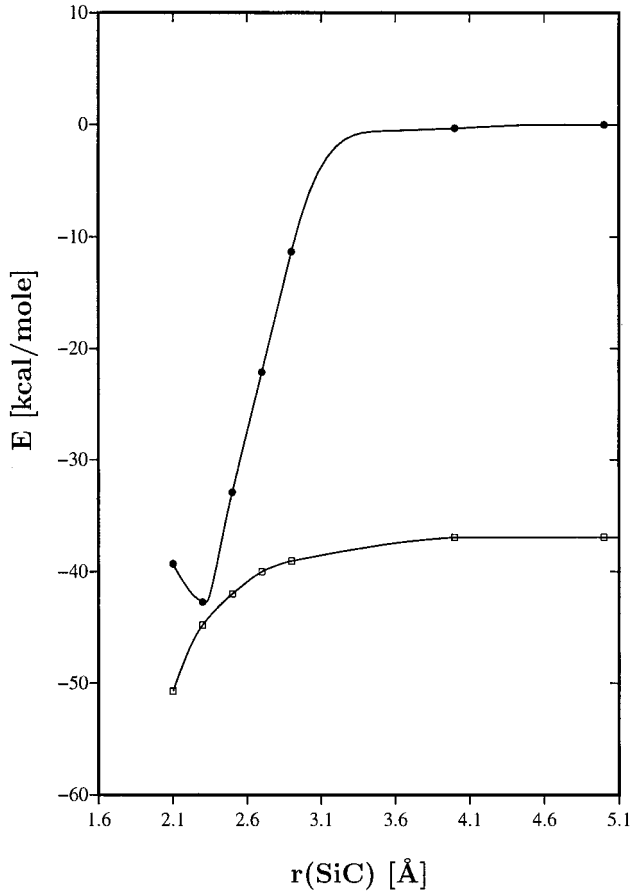


**Figure 8.** Energies of the $1^1A'$ (□) and $2^1A'$ states (●) for the $SiH_2(^1B_1)$ + $CH_2SiH_2$ reaction along the minimum energy path for the attack of silylene at the carbon center. For more information see Figure 5.

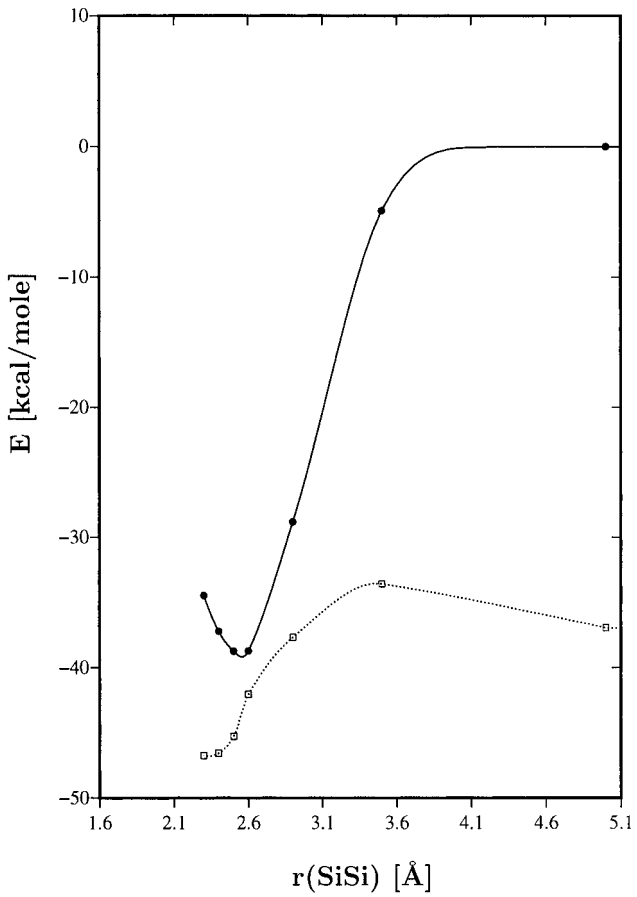


**Figure 9.** Energies of the $1^1A'$ (□) and $2^1A'$ states (●) for the $SiH_2(^1B_1)$ + $CH_2SiH_2$ reaction along the minimum energy path for the attack of silylene at the silicon center. For more information see Figure 5.

of the higher level correction can be seen if the estimated higher correction is compared with the difference between the accurate MR-CI value given by Bauschlicher et al. (19.54 kcal/mol) and the QCISD(T) value (18.0 kcal/mol). The difference gives a correction of 1.54 kcal/mol, while the higher order correction estimated within the G2 theory predicts a deficiency of 3.1 kcal/mol. Keeping in mind that the description of the singlet−triplet gap in silylene is quite complicated, we expect similar errors bars for the bonding energies.

Trends in the stabilities of the three-membered rings were already discussed by Horner et al.[6] and Al−Rubaiey et al.[10] The former computed the stabilization energies using the CCSD/6-31G* approach. For an explanation of the trends, they employed a simple model in which the building reaction of the three-membered rings is divided into the successive formation of two new bonds, which is accompanied by the breaking of the $\pi$ bond of ethene or silene. Further considered is the ring strain of the product, which diminishes the stabilization energy and the divalent state stabilization energy (DSSE) first defined by Walsh.[24] The DSSE is used to account for the difference in the $H_2X-YH_3$ and $H_3X-YH_3$ bond dissociation energies. A good review about the influence of the DSSE on the chemical properties of carbon-, silicon-, and germanium-containing compounds is given by Grev.[25] Using the method described above, the stabilization energy $\Delta E$ can be estimated in terms of contributions from single-bond dissociation energies, strain energies, $\pi$ bond energies, and the DSSE.

$$\Delta E(^1A_1) \approx -D(XH_3-YH_3) - D(XH_3-ZH_3) + \text{strain energy} + D_\pi(H_2Y{=}ZH_2) + \text{DSSE}(XH_2) \quad (1)$$

The values obtained by Horner et al. are also given in Table 1 while the data used to estimate the stabilization energies are summarized in Table 3.

As pointed out previously,[6] this model reproduces the trends in the stabilization energies. Differences between the methylene and the silylene reactions result from differences in the DSSE of $SiH_2$ and $CH_2$ (+19.3 vs −14.6 kcal/mol) and the strain energies of the products (35.2 vs 28.1 kcal/mol), while the difference between the Si−C and the C−C single-bond energies (88.2 vs 89.9 kcal/mol) is not significant. The differences between the silene and the ethene reactions result from the $\pi$ bond strength in silene and ethene (38 vs 65 kcal/mol) and the weaker Si−Si single bond compared to the C−Si single bond (73.6 vs 88.2 kcal/mol).

The model can also be used to rationalize the stabilization energies of the triplet reactions if the singlet−triplet gap (ST−gap) defined as $E(^3B_1) - E(^1A_1)$ is taken into account:

$$\Delta E(^3B_1) \approx -D(XH_3-YH_3) + D_\pi(H_2Y{=}ZH_2) + \text{DSSE}(XH_2) - (\text{ST-gap}) \quad (2)$$

The ST-gaps are −8.6 kcal/mol for methylene and +20.6 kcal/mol for silylene,[22,23] reflecting the well-known inversion of the energetical sequence of the $^1A_1$ and the $^3B_1$ states of silylene as compared to methylene. As a consequence, the difference between the stabilization energies of the triplet reactions of methylene and silylene with ethene is much smaller than their singlet counterparts, but the methylene stabilization energy is still larger than that of silylene (−35 vs −16 kcal/mol).

**TABLE 1: Energetics of the Reactions Computed in the Present Work. All Values Are Given in kcal/mol**

| | $\Delta E^a$ | $\Delta E^{G2}(0K)^b$ | Horner et al.[c] | est[d] | expt[e] | barrier |
|---|---|---|---|---|---|---|
| $CH_2(^1A_1) + C_2H_4 \rightarrow C_3H_6(^1A_1)$ | −106[f] | −100 | −107 | −101 | −102 | |
| $SiH_2(^1A_1) + C_2H_4 \rightarrow SiC_2H_6(^1A')$ | −44 | −42 | −48 | −57 | −47 | |
| $SiH_2(^1A_1) + CSiH_4 \rightarrow Si_2CH_6(^1A')$ | −61 | −61 | −61 | −67 | | |
| $CH_2(^3B_1) + C_2H_4 \rightarrow C_3H_6(^3A_1)$ | −35[f] | −29 | | −31 | | 7 |
| $SiH_2(^3B_1) + C_2H_4 \rightarrow SiC_2H_6(^3A_1')$ | −16 | −14 | | −24 | | 2 |
| $SiH_2(^3B_1) + CSiH_4 \rightarrow$ (sym.)$Si_2CH_6(^3A')$ | −46 | −45 | | −54 | | |
| $SiH_2(^3B_1) + CSiH_4 \rightarrow$ (asym.)$Si_2CH_6(^3A')$ | −37 | −39 | | −40 | | |
| $SiH_2(^1B_1) + C_2H_4 \rightarrow SiC_2H_6(2^1A')$ | −22 | *g* | | | | |
| $SiH_2(^1B_1) + CSiH_4 \rightarrow$ (sym.)$Si_2CH_6(2^1A')$ | −43 | *g* | | | | |
| $SiH_2(^1B_1) + CSiH_4 \rightarrow$ (asym.)$Si_2CH_6(2^1A')$ | −36 | *g* | | | | |

[a] Computed stabilization energies using the MR-CI(18) approach in combination with a 6-311G** AO basis set. [b] Computed stabilization energies using the G2 theory[17] and including the zero-point energy correction obtained on the HF/6-31G* level. [c] CCSD/6-31G* computations; see ref 6. [d] Estimated using eqs1 and 2. For more explanation, see text. [e] Estimated from measurements of the absolute rate constant; see ref 10. [f] See ref 18. [g] The G2 method is not usable for the $^1B_1$ reaction because the products possess strong multireference effects that cannot be described within the G2 method.

**TABLE 2: Minimum Structures of the Silylene Reactions with Ethene (X = C) and Silene (X = Si)[a]**

| | ethene | | | silene | | | | |
|---|---|---|---|---|---|---|---|---|
| | $^3B_1$ | $^1A_1$ | $^1B_1$ | $^3B_1$ symm | $^3B_1$ asymm | $^1A_1$ | $^1B_1$ symm | $^1B_1$ asymm |
| ∠(SiCX) | 115 | 65 | 105 | 116 | | 73 | 110 | |
| ∠(CSiX) | | 50 | | | | 54 | | |
| ∠(CXSi) | | 65 | | | 116 | 54 | | 96 |
| *r*(CSi) | 1.96 | 1.88 | 2.20 | 1.92 | | 1.94 | 2.30 | |
| *r*(CX) | 1.52 | 1.88 | 1.47 | 1.92 | 1.89 | 1.94 | 1.80 | 1.79 |
| *r*(SiX) | | 1.59 | | | 2.39 | 2.30 | | 2.50 |
| $\beta_1$ | 117 | 113 | 117 | 109 | 108 | 112 | 110 | 108 |
| $\beta_2$ | 108 | 113 | 113 | 107 | 116 | 112 | 111 | 116 |
| $\beta_3$ | 109 | 113 | 112 | 109 | 110 | 113 | 108 | 108 |
| $\alpha_1$ | 54 | 39 | 44 | 51 | 56 | 37 | 50 | 56 |
| $\alpha_2$ | 18 | 39 | 26 | 58 | 0 | 36 | 42 | 0 |
| $\alpha_X$ | 51 | 0 | 80 | 52 | −45 | 16 | 94 | 90 |
| $\gamma_1$ | | 141 | | | | 143 | | |
| $\gamma_2$ | | 141 | | | | 144 | | |
| $\gamma_3$ | | 155 | | | | 142 | | |
| *r*(C−H) | 1.09 | 1.08 | 1.09 | 1.09 | 1.08 | 1.08 | 1.08 | 1.08 |
| *r*(Si−H) | 1.48 | 1.47 | 1.48 | 1.48 | 1.48 | 1.47 | 1.48 | 1.48 |
| *r*(X−H) | 1.08 | 1.08 | 1.07 | 1.48 | 1.48 | 1.47 | 1.48 | 1.48 |

[a] For the $^3B_1$ and the $^1B_1$ reactions with silene, the minimum structures of the asymmetric and the symmetric product are given. Distances in angstroms.

**TABLE 3: Data Used for the Estimated Stabilization Energies[a]**

| | |
|---|---|
| $H_3X-YH_3$ Dissociation Enthalpy | |
| $D(H_3C-CH_3)$ | 89.9 [30] |
| $D(H_3C-SiH_3)$ | 88.2 [29] |
| $D(H_3Si-SiH_3)$ | 73.6 [29] |
| Divalent State Stabilization Energies | |
| $SiH_2(^1A_1)$ | 19.3 [25] |
| $CH_2(^1A_1)$ | −14.6 [25] |
| Singlet−Triplet Gap $E(^3B_1) - E(^1A_1)$ | |
| $CH_2$ | −8.6 [32] |
| $SiH_2$ | 21.0 [22] |
| Strain Energies | |
| c-$C_3H_6$ | 28.1 [6] |
| c-$SiC_2H_6$ | 35.2 [6] |
| c-$Si_2CH_6$ | 37.0 [6] |
| $\pi$ Bonding Enthalpy | |
| $H_2C{=}CH_2$ | 65 [31] |
| $H_2C{=}SiH_2$ | 38 [31] |

[a] Energies in kcal/mol. Reference in brackets.

As discussed in the previous sections, the minima for the $^1B_1$ reactions of silylene are found at long Si−C (2.3 Å) and Si−Si (2.6 Å) distances where the new bonds are not fully formed. However, a comparison between the $^3B_1$ and the $^1B_1$ reactions shows that the stabilization energies of the corresponding reactions are very similar. These unexpectedly strong stabilization energies of the $^1B_1$ reaction may be explained by the character of the electronic wave function at the minimum of the $^1B_1$ PES, which represents a mixture between the $^1A_1$ and the $^1B_1$ character.

**Photochemical Relevance of the $^1B_1$ Reactions.** In the $^1B_1$ products, a charge accumulation on the attacking silylene fragment is accompanied by a charge depletion on the second terminal center. Therefore, both electrophilic and nucleophilic reactions could follow the $^1B_1$ reaction. However, another process competing with these reactions is the internal conversion from the electronically excited $2^1A'$ PES to the electronic ground state $1^1A'$, which results from the avoided crossing between both low-lying singlet states. The MEP including the avoided crossings are given in Figures 4, 8, and 9. To obtain a rough estimate for the efficiency of the internal conversion the following model is used:

1. The attack of the silylene fragment can be approximated by the MEP, i.e., by a one-dimensional model using $r_{SiX}$ as reaction coordinate.

2. The excess energy gained due to the stabilization energy of the $^1B_1$ reaction is partially distributed to other nuclear degrees of freedom (IVR).[26] To simulate this effect the energy of the collision complex was set equal to 90% and 50% respectively of the stabilization energy of the $^1B_1$ reactions.

3. Molecules that perform an internal conversion to the $1^1A'$ ground state do not cross back to the excited state but give vibrationally highly excited ground-state products. Two reasons for this assumption are the form of the ground-state PES, which in the crossing region possesses large-energy gradients pointing to the cyclic equilibrium geometry of the ground state, and the redistribution of the excess energy to the other internal degrees of freedom, which is known to be a fast process.[26]

4. The diabatic coupling matrix element is estimated as half of the minimal energy separation of both adiabatic surfaces

$$H_{12} = -{}^1/_2(E^{1^1A'}(R_x) - E^{2^1A'}(R_x)) \qquad (3)$$

with $R_x$ being the crossing point of the diabatic potential curves.

Within this model the nonadiabatic transition probability by one passage of the crossing point is given by the Landau−Zener transition probability, *p*,[27] which we used in the form given by Zhu and Nakamura[28]

$$p = \exp\left\{-\frac{\pi}{4ab}\left[\frac{2}{1+\sqrt{1+b^{-4}g_5}}\right]^{1/2}\right\} \qquad (4)$$

with $g_5 = 0.72 - 0.62a^{1.43}$.

**TABLE 4: Coupling Matrix Element between Both Diabatic Curves ($H_{12}$) and the Landau−Zener Transition Probability $p$ (For More Explanation See Text)**

| | | $p$ | |
|---|---|---|---|
| reaction | $H_{12}$ (au) | 90%[a] | 50%[a] |
| $SiH_2 \rightarrow H_2C{=}CH_2$ | 0.000 38 | 0.99 | 0.98 |
| $SiH_2 \rightarrow H_2C{=}SiH_2$ | 0.0015 | 0.95 | 0.94 |
| $SiH_2 \rightarrow H_2Si{=}CH_2$ | 0.0027 | 0.74 | 0.69 |

[a] Estimating $E - E_x$ by 90% and 50% of the stabilization energy of the $^1B_1$ reaction. Stabilization energies are given in Table 1.

In the diabatic representation $a$ and $b$ are defined as

$$a^2 = \frac{\hbar^2}{2m}\frac{F(F_1 - F_2)}{8V_x^3} \qquad b^2 = (E - E_x)\frac{F_1 - F_2}{2FV_x} \quad (5)$$

where $m$ represents the reduced mass and $F = (|F_1F_2|)^{1/2}$. $F_i$ ($i$ = 1,2), $V_x$, and $E_x$ represent the slopes of the diabatic surfaces, the diabatic coupling, and the energy, respectively. They are defined at the crossing point ($R = R_x$). $E$ represents the total energy of the collision complex, and as already discussed above, to simulate IVR effects we used 90% and 50% respectively, of the $^1B_1$ stabilization energies given in Table 1 for $E - E_x$. The results are summarized in Table 4, which contains the coupling matrix element between the diabatic surfaces, the Landau−Zener transition probability $p$ for the internal conversion. The columns labeled with 90% and 50% indicate that we used 90% and 50%, respectively, of the stabilization energy of the $^1B_1$ − reaction for $E - E_x$. The calculated values clearly show that the intersystem crossing is the dominant branch of possible secondary reactions following the $^1B_1$ reactions. For most of the reactions studied, only a single passage of the crossing point is sufficient to depopulate the electronically excited $^1A'$ state by more than 90%. This implies that the main products of the $^1B_1$ reactions will be thermally highly excited ground-state molecules. Because the energy differences between the minima of the $2^1A'$ states and the equilibrium geometries of the ground states are larger than the stabilization energies calculated for the $^1A_1$ reactions, it seems likely that the internal conversion will be followed by fragmentation reactions.

The results of the present study show that the photochemical route via excited singlet silylene does not seem to represent an efficient way to build up larger silicon−carbon compounds.

**The Influence of Intersystem Crossings on the Triplet Reactions.** The overall reaction rate of a reaction starting from a triplet educt state and ending in a singlet product state can be influenced by singlet states in two ways. In the first case, the intersystem crossing to the singlet state takes place after forming the triplet product via the normal triplet reaction mechanism. In the second case, the intersystem crossing happens before the triplet product is formed. If it takes place before possible reaction barriers of the triplet reaction are reached, an acceleration of the overall reaction is found. As shown previously,[18] such a case is found for the $CH_2(^3B_1) + C_2H_4$ reaction, which is influenced by the $^1A_1$ reaction. In contrast, for the reaction of silylene discussed in the present work the first case is found. For the reaction $SiH_2(^3B_1) + SiH_2{=}CH_2 \rightarrow H_2Si{-}H_2C{-}SiH_2$-($^3A'$), this is shown in Figure 10. It contains the MEP of the $^3B_1$ reaction and the energies of the $1^1A'$ and $2^1A'$ states calculated at the optimal triplet geometries. On the MR-CI(6) level in combination with the 6-31G** basis set the triplet state is better described than the $^1A_1$ state, i.e., the ST-gap is calculated by 4.3 kcal/mol too small. To obtain a more reliable description of the influence of the $^1A_1$ reaction channel on the $^3B_1$ reaction, we shifted the triplet PES by this amount. For some points of the PES this approximation was checked on the MR-CI(18) level in combination with the 6-311G** basis set. Figure 10 shows that an intersystem crossing can only take place after the triplet product is formed. For larger values of $r_{SiC}$ the energetical separations of the $^3A'$ and $1^1A'$ states are too large.

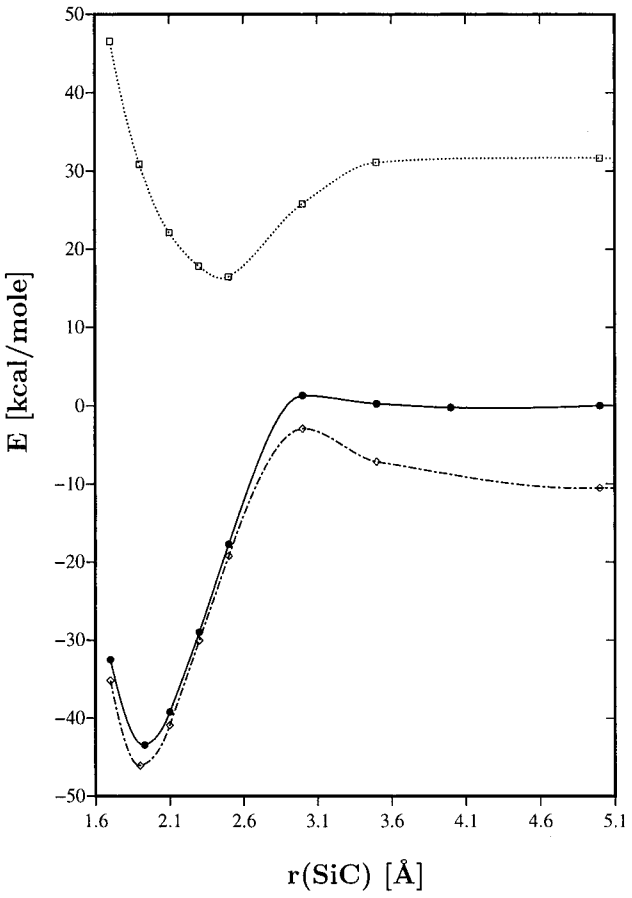


**Figure 10.** Potential energy curves of the electronic states $1^1A'$ (◇), $2^1A'$ (□), and $^3A'$ (●) along the MEP of the $SiH_2(^3B_1) + CH_2SiH_2$ reaction For more information see Figure 2.

The minimum of the triplet state ($^3A'$) lies 32 kcal/mol (11423 $cm^{-1}$) above the minimum of the singlet ground state (cyclic form). As a consequence, the Franck−Condon factors influencing the triplet−singlet intersystem crossing will be small. We therefore expect rather long lifetimes of the triplet products.

Going from the optimal triplet geometries to geometries being optimized for the $^1B_1$ reaction, the energetical sequence of the three states ($1^1A'$,$^3A'$,$2^1A'$) remains unchanged, i.e., we do not find a crossing of the triplet surface with one of the singlet surfaces in the vicinity of the MEP of the triplet reaction, which could increase the efficiency of the intersystem crossing.

For the other triplet reactions discussed in the present paper, a similar situation is found.

## 4. Summary

In the present work the photochemical behavior of silylene ($SiH_2$) is studied. The PESs governing the reactions of $SiH_2$ in its first two excited states ($^3B_1$ and $^1B_1$) with ethene and silene are calculated, and the internal conversion from the excited singlet state to the electronic ground state is estimated using the Landau−Zener model. For all reactions we find that the $^1B_1$ reaction is strongly influenced by an avoided crossing with the electronic ground state. This avoided crossing leads to unusual equilibrium geometries of the first excited singlet state and is the reason for a large nonadiabatic coupling between both states. Due to the strong coupling our calculations suggest that

the internal conversion is the dominant branch of possible secondary reactions following the $^1B_1$ reaction. In contrast to the $^1B_1$ reactions, no crossing with both singlet surfaces is found in the vicinity of the MEP of the $^3B_1$ reactions. Since the Franck−Condon factors influencing the singlet−triplet intersystem crossing will be small, we expect rather long lifetimes of the triplet products.

For comparison the ground-state reactions [ $SiH_2(^1A_1) + C_2H_4/SiCH_4$ ] are also presented in the present work. For the reaction with silene we find a similar reaction mechanism as described for the reaction of silylene($^1A_1$) with ethene.[5]

## References and Notes


(1) Jasinski, J. M.; Meyerson, B. S.; Scott, B. A. *Annu. Rev. Phys. Chem.* **1987**, *38*, 109.

(2) Bauschlicher, C. W.; Taylor, P. R. *J. Chem. Phys.* **1987**, *86*, 1420.

(3) Winter, C.; Millie, P.; *Chem. Phys.* **1993**, *174*, 177.

(4) Handy, J. E.; Rice, N. C. *Chem. Phys. Lett.* **1987**, *107*, 365.

(5) Anwari, F.; Gordon, M. S. *Isr. J. Chem.* **1983**, *23*, 129.

(6) Horner, D. A.; Grev, R. S.; Schaeferm H. F., III, *J. Am. Chem. Soc.* **1992**, *114*, 2093.

(7) Rogers, D. S.; Walker, K. L.; Ring, M. A.; O'Neal, H. E. *Organometallics* **1987**, *6*, 2313.

(8) Chu, J. O.; Beach, D. H.; Jasinski, J. M. *J. Phys. Chem.* **1987**, *91*, 5340.

(9) Inoue, G.; Suzuki, M. *Chem. Phys. Lett.* **1985**, *122*, 361.

(10) Al−Rubaiey, N.; Frey, H. M.; Mason, B. P.; McMahon, C.; Walsh, R. *CPL* **1993**, *204*, 301.

(11) Apeloig, Y. *The Chemistry of Organic Silicon Compounds*; Patei, S., Rappoport, Z., Eds.; John Wiley & Sons: New York, 1989; pp 57−227.

(12) Shepard, R. *Adv. Chem. Phys., 69, Ab Initio Methods in Quantum Chemistry*; Rice, S. A., Ed.; John Wiley and Sons: New York, 1987; Vol. II, pp 63−200.

(13) Werner, H.-J. *Adv. Chem. Phys., 69, Ab Initio Methods in Quantum Chemistry*; Rice, S. A., Ed.; John Wiley and Sons: New York, 1987; Vol. II, pp 1−65.

(14) MOLPRO is a package of ab initio programs written by H.-J., Werner, and P. J., Knowles with contributions from Almlöf, J.; Amos, R. D.; Deegan, M. J. O.; Elbert, S. T.; Hampel, C.; Meyer, W.; Peterson, K.; Pitzer, R.; Stone, A. J.; Taylor, P. R.

(15) Carbon: (sp) Hehre, W. J.; Ditchfield, R.; Pople, J. A. *J. Chem. Phys.* **1972**, *56*, 2257; (d) Huzinaga, S. *Chem. Phys.* **1965**, *42*, 1293. Silicon: (sp) Francl, M. M.; Pietro, W. J.; Hehre, W. J.; Binkley, J. S.; Gordon, M. S.; Defrees, D. J.; Pople, J. A. *Chem. Phys.* **1982**, *77*, 3654; (d) Whitman, D. R.; Hornback, C. J. *J. Chem. Phys.* **1969**, *50*, 1371. Hydrogen: Krishnan, R.; Binkley, J. S.; Seeger, R.; Pople, J. A. *J. Chem. Phys.* **1980**, *72*, 650.

(16) Carbon: (spd) Krishnan, R.; Binkley, J. S.; Seeger, R.; Pople, J. A. *J. Chem. Phys.* **1980**, *72*, 650. Silicon: (sp) Mclean, A. D.; Chandler, G. S. *J. Chem. Phys.* **1980**, *72*, 5639; (d) Francl, M. M.; Pietro, W. J.; Hehre, W. J.; Binkley, J. S.; Gordon, M. S. Defrees, D. J.; Pople, J. A. *Chem. Phys.* **1982**, *77*, 3654. Hydrogen: Krishnan, R.; Binkley, J. S.; Seeger, R.; Pople, J. A. *J. Chem. Phys.* **1980**, *72*, 650.

(17) Curtiss, L. A.; Rhaghavachari, K. *Calculations of Accurate Bond Energies, Understanding Chemical Reactivity*; Langhoff, S. R., Ed.; Kluwer Academic Publishers: Dordrecht, 1995; Vol. 13, pp 139−172.

(18) Reuter, W.; Engels, B.; Peyerimhoff, S. D. *J. Phys. Chem.* **1992**, *96*, 6221.

(19) Boatz, J. A.; Gordon, M. S. *J. Phys. Chem.* **1989**, *93*, 3025.

(20) Zurawski, B.; Kutzelnigg, W. *J. Am. Chem. Soc.* **1978**, *100*, 2654.

(21) Hildebrandt, H. Diplomarbeit, Bonn, 1996. Lennartz, Ch. Diplomarbeit, Bonn, 1996.

(22) Bauschlicher, C. W.; Langhoff, S. R.; Taylor, P. R. *J. Chem. Phys.* **1987**, *87*, 387.

(23) Berkowitz, J.; Greene, J. P.; Cho, H.; Ruščić, B. *J. Chem. Phys.* **1987**, *86*, 1235.

(24) Walsh, R. *Acc. Chem. Res.* **1981**, *14*, 246.

(25) Grev, R. S. *Adv. Org. Met. Chem.* **1991**, *36*, 125.

(26) Geers, A.; Kappert, J.; Temps, F.; Wiebrecht, J. *J. Chem. Phys.* **1994**, *101*, 3634.

(27) (a) Landau, L. D. *Phys. Z. Sowjetunion 2* **1932**, 46. (b) Zener, C. *Proc. R. Soc. London Ser. A B7*, **1932**, 696.

(28) Zhu, C.; Nakamura, H. *J. Chem. Phys.* **1995**, *102*, 7448.

(29) Walsh, R. *The Chemistry of Organic Silicon Compounds*; Patai, S., Rappoport, Z., Eds.; Wiley: New York, 1989; Chapter 5.

(30) Wagman, D. D.; Evans, W. H.; Parker, V. B.; Schumm, R. H.; Halow, I.; Bailey, S. M.; Churney, K. L.; Nuttal, R. L. The NBS Table of Chemical Thermodynamic Properties. *J. Phys. Chem. Ref. Data* **1982**, *11*, Suppl. 2.

(31) Schmidt, M. W.; Truong, P. N.; Gordon, M. S. *J. Am. Chem. Soc.* **1987**, *112*, 5217.

(32) McKellar, A. R. W.; Bunker, P. R.; Sears, T. J. Evenson, K. M.; Saykally, R. J.; Langhoff, S. R. *Chem. Phys.* **1983**, *79*, 5251.